Journal of Mining and Geology Vol. 57(2) 2021. pp. 351 - 364 0022-2763

Groundwater Investigation Across the Crystalline Basement Rocks in Rogo Area, Kano State Northern Nigeria, Using Resistivity Methods

Anudu, G.K.[1,2], Obrike, S.E.[1,2] and Ofoegbu, C.O.[2]
[1]Department of Geology and Mining, Nasarawa State University, PMB 1022, Keffi, Nigeria.
[2]Institute of Geosciences and Earth Resources, Nasarawa State University, Keffi, Nigeria.
Corresponding E-mail: **zobrike@gmail.com**

Abstract
One-dimensional (1D) resistivity sounding (VES) and two-dimensional (2D) resistivity imaging methods were employed in groundwater investigation in order to delineate potential aquifers and estimate their transmissivities in Rogo area. Main basement rock units in the area are granites and schistose quartzite rocks of Precambrian to Lower Paleozoic age. Twelve resistivity soundings (VES) were carried out across the area using Schlumberger electrode configuration. The field resistivity sounding data obtained were interpreted with partial curve matching approach and 1D inversion algorithm, IPI2Win. The 2D resistivity imaging survey was conducted along two traverses employing dipole-dipole electrode configuration and the resistivity data acquired were subjected to finite element method modelling using DIPRO inversion algorithm to generate a geologically realistic, 2D subsurface geological model. Three to five geoelectrical layers, as well as weathered bedrock (saprolite) and fractured bedrock (saprock) aquifers were delineated. Seven resistivity sounding curve types (namely H, HA, HK, KH, QH, HKH and KQH) were also identified with the H and HA types being the dominant curve types. Anisotropy coefficient (λ) values ranged from 1.03 to 2.65 with a mean of 1.31. Aquifer transmissivity computed for the weathered bedrock aquifer units varied from 16.01 to 53.3 m^2/day, with an average value of 30.91 m^2/day. The study revealed that the Rogo area has moderately high aquifer transmissivity and hence generally exhibits good groundwater potentials.

Keywords: *1D resistivity sounding (VES), 2D resistivity imaging, aquifer, aquifer transmissivity, anisotropy coefficient, Rogo.*

Introduction

Rogo area, comprised of different rural communities in Kano State, is situated on the crystalline basement rocks of northern Nigeria which are Precambrian to Lower Paleozoic in age. It is witnessing an upsurge in human population and agricultural activities because of its proximity to Zaria, a major and oldest city in Kaduna State. This has resulted in generation of more domestic and agricultural wastes which are disposed into the surface water bodies, and such uncontrolled disposal method can result in pollution and/or contamination of the surface water resources in the area. At present, the populace and establishments are dependent upon the few surface water resources as well as on groundwater abstracted from few hand-dug wells and/or motorized hand-pump boreholes for their domestic and agricultural uses. Therefore the demand for potable water for domestic and agricultural uses has grown astronomically over the years.

Crystalline basement complex rocks, in general, have low to negligible porosity and permeability and thus, are often hydrogeologically considered to be poor aquifers. However, they typically exhibit moderate to moderate porosity and permeability when weathered and/or fractured, and in such case can be good aquifers. Therefore, groundwater occurrences and availability in the Precambrian to Lower Paleozoic crystalline basement complex rocks across Nigeria are generally due to development of secondary porosity and permeability resulting from weathering and fracturing (e.g. Olayinka and Olorunfemi, 1992; Anudu *et al*., 2008, 2011, 2014). The weathering profile above crystalline basement rocks in low latitude and/or tropical regions (Wright, 1992; Taylor and Eggleton, 2001) could be describe, from top to bottom, as follows: (1) collapsed zone derived from prolonged dissolution and leaching of weathered bedrock and usually has a negligible thickness. It is composed of the soil/mobile zone, duricrust and mottled zone. It is usually clayey, silty, sandy and/ lateritic in nature depending on the chemistry and mineralogy of the parent bedrock; (2) weathered bedrock (saprolite) formed from prolonged in situ weathering or decomposition of the bedrock. It is few meters to tens of meters thick and is usually aquiferous in nature; (3) fractured bedrock (saprock) derived from extensive fracturing and slight in situ weathering of bedrock. It is characterized by sub-vertical and sub-horizontal fracture sets which most of the time are juxtaposed and also aquiferous in character, and (4) fresh bedrock which has very little or no fractures. A typical field example observed in the study area is shown in Figure 1. Generally, the intensity of weathering, density of fractures and degree of fracture interconnectivity decrease with increase in depth.

Aquifers occur within the highly weathered bedrock (saprolite) and fractured bedrock (saprock) zones in the Precambrian to Lower Paleozoic crystalline basement rocks (e.g. Olayinka and Olorunfemi, 1992; Olorunfemi and Fasuyi, 1993; Olayinka *et al*., 1997; Dan-Hassan

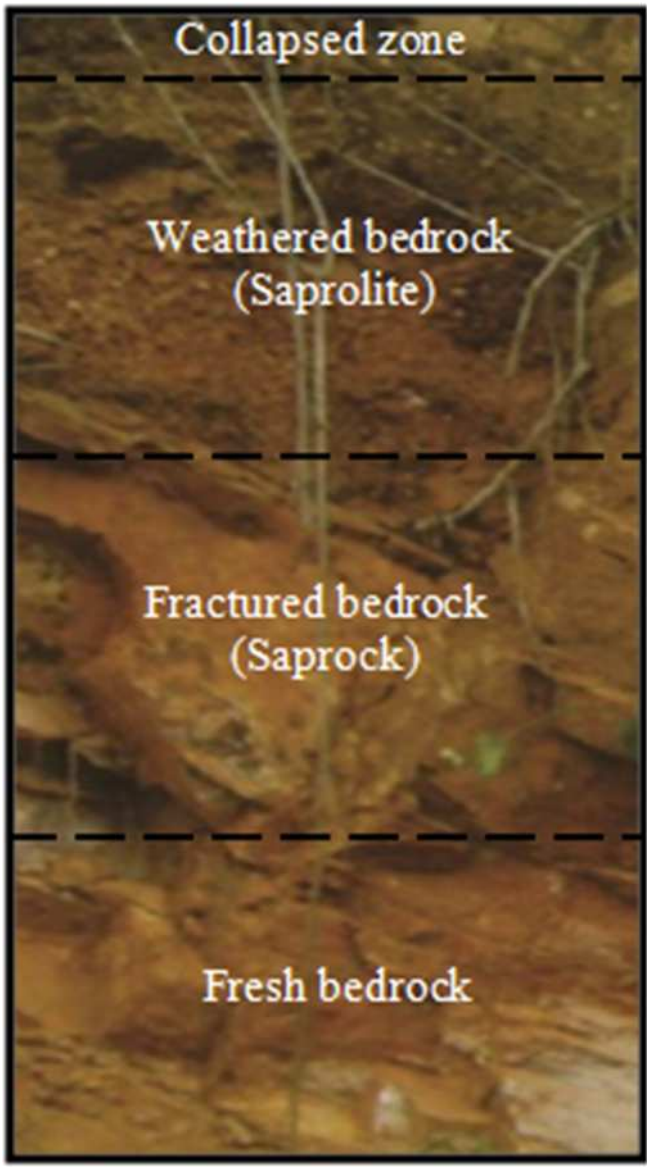

Fig. 1: Weathering profile observed on a schistose quartzite rock at Tsohuwar-Rogo in the area.

and Olorunfemi, 1999; Anudu *et al*., 2008, 2011, 2014). The crystalline basement aquifers are usually variable and discontinuous in nature and therefore detailed knowledge of the subsurface geology, hydrogeological and geophysical investigations are inevitable. Resistivity methods are the most popular of geophysical methods for groundwater investigation because they often give a strong response to subsurface conditions and are relatively cost-effective (Ernstson and Kirsch, 2006). The vertical electrical sounding (VES) (also referred to as 1D resistivity sounding) and 2D resistivity imaging techniques of the resistivity methods have proved very useful especially for the delineation of weathered and fractured zones in the Precambrian to Lower Paleozoic crystalline basement rocks of Nigeria (e.g. Olayinka and Olorunfemi, 1992; Olorunfemi and Fasuyi, 1993; Olayinka *et al*., 1997; Dan-Hassan and Olorunfemi, 1999; Anudu *et al*., 2008, 2011, 2014).

Many articles have been published on groundwater investigation in the Nigerian crystalline basement complex, employing vertical electrical sounding (VES) technique of the resistivity methods (e.g. Offodile, 1983; Barongo and Palacky, 1991; Olayinka and Olorunfemi, 1992; Olorunfemi and Fasuyi, 1993; Aina *et al*., 1996; Olayinka, 1996; Olayinka *et al*., 1997; Dan-Hassan and Olorunfemi, 1999; Bala and Ike, 2001; Anudu *et al*., 2008, 2011, 2014). Geoelectrical succession in the Precambrian to Lower Paleozoic crystalline basement terrains of Nigeria usually consist of a thin (0 to 2 m) highly resistive collapsed zone (with resistivity ranging from 100 to 4000 ohm-m), a highly conductive weathered bedrock (having resistivity varying from 10 to 200 ohm-m with thickness lower than 50 m) and a highly resistive crystalline bedrock whose resistivity exceeds 1000 ohm-m (Aina *et al*., 1996; Olayinka, 1996; Olayinka *et al*., 2000). The fractured bedrock resistivity is generally lower than 1500 ohm-m (David, 1988; Hazell *et al*., 1992) but can be up to 3000 ohm-m (White *et al*., 1988). According to Olayinka (1996), crystalline bedrocks having resistivity surpassing 3000 ohm-m usually depict fresh bedrocks with little or no water. Highest groundwater yields from deep water wells or boreholes in the Precambrian to Lower Paleozoic crystalline basement rocks are found in zones where fractured bedrocks (saprocks) occur directly beneath thick weathered bedrocks (saprolites) (Anudu, *et al*., 2008, 2011, 2014).

Aquifer parameters such as transmissivity (T) and hydraulic conductivity (K) are usually determined for boreholes and/or deep wells during hydrogeological investigations using pumping test methods; this method is time consuming and expensive. However in areas with limited or few pumping test data, aquifer transmissivity and hydraulic conductivity could be estimated from vertical electrical sounding (VES) technique of resistivity methods. This technique is simpler, faster and cost effective. Several workers had used resistivity sounding (VES) techniques to estimate aquifer transmissivity and hydraulic conductivity in different geological terrains all over the world (Kosinki and Kelly, 1981; Niwas and Singhal, 1981, 1985; Frohlich and Kelly, 1985; Ahmed *et al*., 1988; Onuoha and Mbazi, 1988; Mbonu *et al*., 1991; Mbipom *et al*., 1996; Yadav and Abolfazli, 1998; De Lima and Niwas, 2000; Umego *et al*., 2000; Hubbard and Rubin, 2002; Niwas and De Lima, 2003; Dhakate and Singh, 2005;

Akaolisa, 2006; Soupios *et al*., 2007; Chandra *et al*., 2008).

The present study was focused on investigating the groundwater potential of the crystalline basement rocks in Rogo area using 1D resistivity sounding (VES) and 2D resistivity imaging methods. Its purpose was to ascertain, delineate and evaluate the potential basement aquifers in the area. Thus this study showed the usefulness of electrical resistivity methods in delineating and characterising potential basement aquifers in the Rogo area. This study is novel as there has been no record regarding this aspect of research in the area.

Physical Setting and Geology

The Rogo area is located in the Rogo Local Government Area of Kano State, northern Nigeria. It is situated within latitudes 11o 21'N to 11o 40'N and longitudes 7o38'E to 7o55'E (Figure 2). The area has a tropical climate which is characterized by two seasons: the rainy and dry seasons. The rainy season lasts from April to October, whereas the dry season lasts between November and March. Hamattan is usually experienced from November to February. The mean annual rainfall varies from 600 to 1200 mm, and the mean annual temperature ranges from 32 to 36 oC (Adefolalu, 2002). It falls within the northern Guinea savannah and Sudan savannah vegetation belts of Nigeria (Olorode, 2002).

Geologically, it is situated on the Precambrian to Lower Paleozoic crystalline basement complex of northern Nigeria. It is underlain mainly by granitic gneisses, quartzite/schistose rock, medium to coarse grained biotite granite and porphyritic biotite granite. The granitic gneisses are group under the Precambrian migmatite-gneiss complex rocks; quartzite/schistose rocks are Precambrian metasedimentary rocks, whereas the medium to coarse grained biotite granite and porphyritic biotite granite belong to the Lower Palaeozoic Older Granites or Pan-African granitiods (NGSA, 2009).

Field observations conducted across the study area showed that the basement rocks are highly fractured and/or weathered in most areas, and that groundwater occurs within the weathered bedrock (saprolite) and fractured bedrock (saprock) zones. Additionally, most of the existing hand-dug wells in the area are abstracting water from the weathered bedrock (saprolite) aquifers. These aforementioned observations are similar to several published findings previously observed across most crystalline basement complex terrains of Nigeria (e.g. Offodile, 1983; Barongo and Palacky, 1991; Olayinka and Olorunfemi, 1992; Olorunfemi and Fasuyi, 1993; Aina *et al*., 1996; Olayinka, 1996; Olayinka *et al*., 1997; Dan-Hassan and Olorunfemi, 1999; Bala and Ike, 2001; Anudu *et al*., 2008, 2011, 2014).

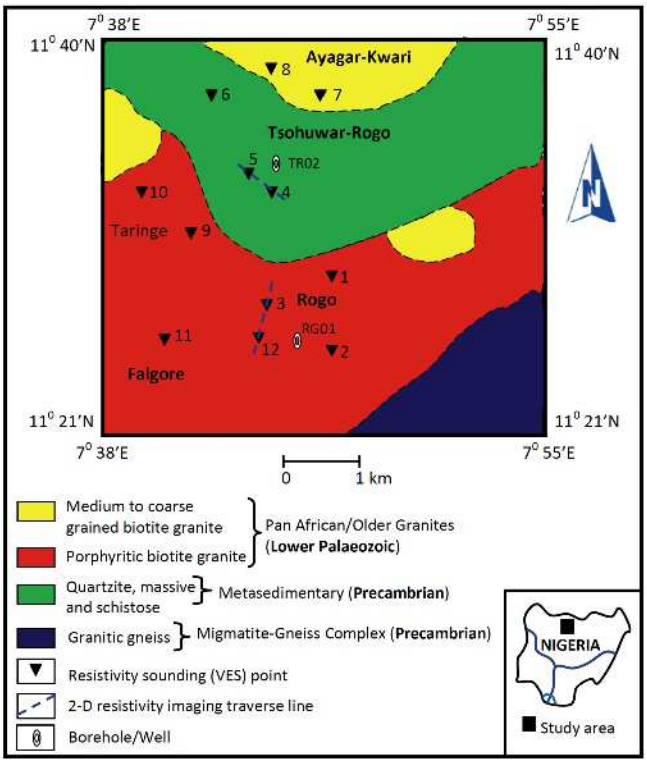

Fig. 2: Geological map of Rogo area (Modified from Nigeria Geological Survey Agency, 2009). Superimposed on it are the resistivity sounding (VES) points, 2-D resistivity imaging traverse lines and borehole/well locations.

Electrical Resistivity Data Acquisition and Processing

Electrical resistivity survey involves the injection of electrical current into the subsurface through two point current electrodes and measurement of the potential difference generated using another two point potential electrodes (e.g. Telford *et al*., 1998; Ernstson and Kirsch, 2009; Reynolds, 2011). Three most widely utilised electrode configuration for electrical resistivity surveys for groundwater investigations or solving hydrogeological problems are Wenner, Schlumberger and dipole-dipole configurations; the first two aforementioned ones (i.e. Wenner and Schlumberger configurations) are typically used for vertical electrical sounding (VES) surveys (also referred to as 1D resistivity sounding), whereas the later (i.e. dipole-dipole configuration) for two-dimensional (2D)

resistivity imaging (e.g. Telford *et al*., 1998; Ernstson and Kirsch, 2009; Janik and Krummel, 2009; Reynolds, 2011). For this present study, the Schlumberger electrode configuration (Figure 2) was adopted for resistivity sounding (VES) surveys because it is moderately sensitive to lateral inhomogeneities and gives a good vertical resolution of the subsurface layers, whereas the dipole-dipole electrode configuration (Figure 3) was employed for the 2D resistivity imaging surveys since it also moderately sensitive to lateral inhomogeneities and produces a good lateral resolution of the subsurface layers as well as has deep depth of penetration (e.g. Reynolds, 2011; Dentith and Mudge, 2014). Resistivity measurements were carried out using the Geopulse Tigre resistivity meter with its accessories manufactured by the Allied Associates Geophysical Limited, England, whose output is resistance.

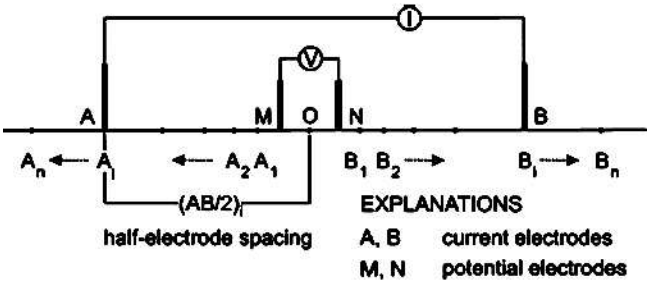

Fig. 2: Schematic Schlumberger configuration for resistivity sounding (VES) survey.

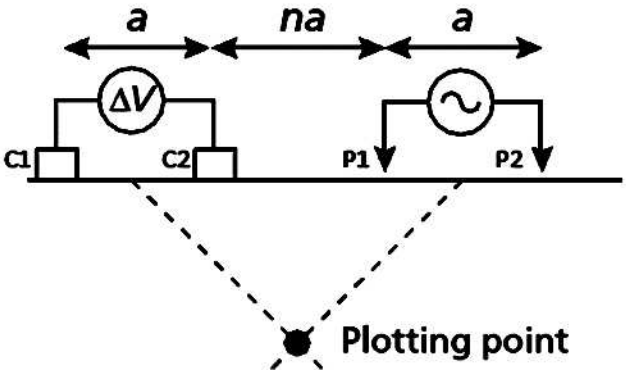

Fig. 3: Schematic dipole-dipole configuration for 2D resistivity imaging measurement.

For the Schlumberger electrode configuration, apparent resistivity (ρ_a) is given as (Zohdy, *et al*. 1974; Gowd, 2004, Batte *et al*., 2008; Anudu *et al*., 2014):

$$\rho a = \pi \left[\frac{\left[\frac{AB}{2}\right]^2 - \left[\frac{MN}{2}\right]^2}{MN} \right] \frac{\Delta V}{I} \quad \text{.....(1)}$$

where, AB/2, MN/2, ΔV, and I are half-current electrode spacing, half-potential electrode spacing, potential difference, and current, respectively. The resistance is the ratio of potential difference and current (i.e. R = ΔV/I).

Twelve (12) vertical electrical soundings (VES) were conducted in the area utilising the Schlumberger electrode configuration and the sounding (VES) points locations are shown on Figure 2. Current electrodes spacing utilised during the resistivity sounding survey were AB = 2, 4, 6, 8, 10, 12, 16, 20, 24, 30, 40, 50, 60, 80, 100, 150, 200, 230 and 300 m; the potential electrodes spacing were MN = 2, 6 and 20 m. When the potential electrode spacing (MN) was increased, readings were taken for the same current electrode spacing (AB) with the previous and expanded MN. Thus, the Schlumberger electrode configuration was gradually expanded at a fixed centre point position along the survey line with half current electrode spacing (AB/2) and half potential electrode spacing (MN/2) varied from 1.5 to 150 m and 1 to 10 m, respectively; which was considered adequate for giving the depth of investigation ranging between 38 and 50 m. Depth of investigation in resistivity sounding employing the Schlumberger electrode configuration is 0.33 to 0.25 of half-current electrode spacing (AB/2) (Roy and Apparao, 1971; Bernard, 2003). During the survey, we aligned the resistivity sounding (VES) points axes parallel to known local and/or regional geological trends so as to reduce the effects of lateral resistivity variations in the subsurface (cf. Ernstson and Kirsch, 2009; Reynolds, 2011). Also some resistivity sounding (VES) points were conducted closer to known, nearby existing water boreholes/wells in order to correlate and constrain the resultant resistivity sounding (VES) data with the available borehole/well lithological log datasets (see Figure 2 for location) as well as to reduce to minimum the ambiguities inherent in the acquired VES results during the data analysis and interpretation stages of this study (cf. Ernstson and Kirsch, 2009; Reynolds, 2011).

The resistivity sounding (VES) data obtained were presented as curves of computed apparent resistivity (ρ_a) against half-current electrode spacing (AB/2) on bi-logarithmic (log-log) graphs, and initial preliminary analysis and interpretations implemented employing the conventional manual partial curve matching approach (e.g. Keller and Frischknecht, 1966; Telford *et al*., 1998; Ernstson and Kirsch, 2009; Reynolds, 2011). Subsequently a 1D inversion algorithm, IPI2Win Version 3.0.1 (Bobachev, 2002), based on Newton-Raphson method and Tikhonov regularization approach, was used to model the initial parameters (resistivity and thickness) obtained from manual analysis and interpretation of each resistivity sounding

data. In order to minimize ambiguity in the interpretation of resistivity sounding (VES) data results related to its non-uniqueness resulting from the inherent equivalence and suppression problems, which show that different input models can produce the same output model curve (e.g. Telford *et al*., 1998; Ernstson and Kirsch, 2009; Reynolds, 2011), available water borehole/well lithological log data in the area (see Figure 2 for location) as well as reasonable geological models were incorporated during the 1D modelling (inversion) tasks. Disregard of either can have a serious negative effect on the validity of the resultant resistivity sounding (VES) data results (i.e. geo-electrical models) for any locality. Thus, the resulting respective models with low root mean square (RMS) error of less than 7.1 % which were obtained after the 1D modelling (inversion) tasks were accepted as the final interpreted geo-electrical models of the subsurface. Representative plots of computed apparent resistivity (ρ_a) versus half-current electrode spacing (AB/2) and the final interpreted geo-electrical models are shown in Figure 3.

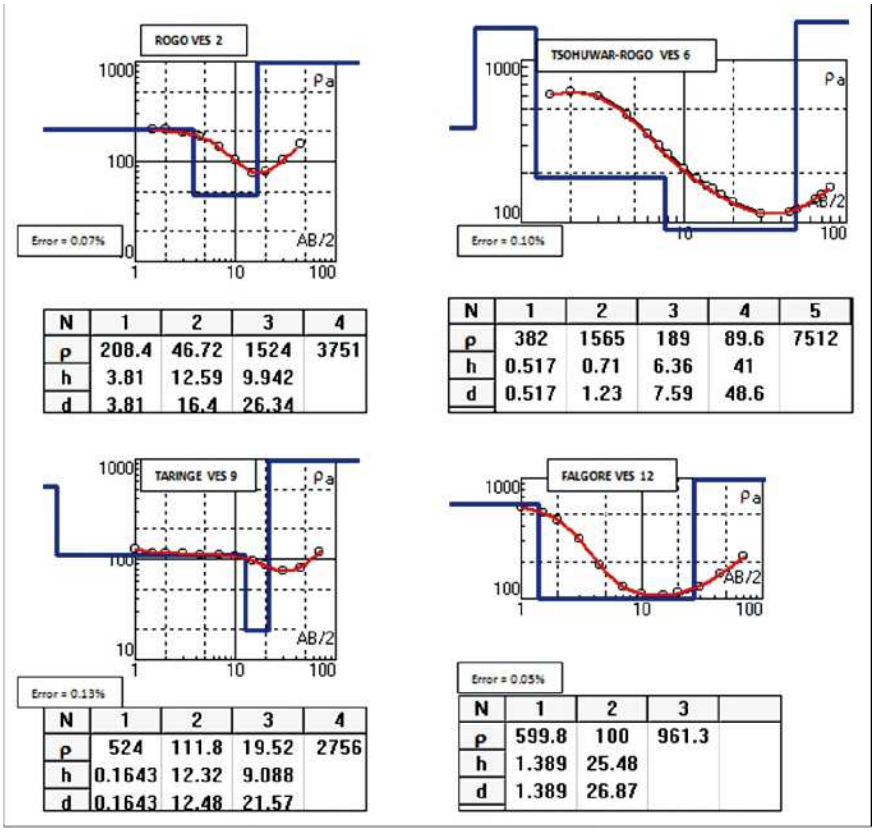

Fig. 3: Representative plots of apparent resistivity (ρa) versus half-current electrode spacing (AB/2) and interpreted geoelectrical models for the Rogo area. N, ρ, h and d are number of layers, resistivity, thickness and depth, respectively.

Table 1: Summary of the vertical electrical sounding (VES) interpretation results for the area.

VES No	No of layers	Curve type	Resistivity of layers (ohm-m)					Thickness of layers (m)				Depth to fresh bedrock (m)
			ρ_1	ρ_2	ρ_3	ρ_4	ρ_5	h_1	h_2	h_3	h_4	
1	4	KH	212.1	258	154	3083	-	1.30	16.31	13.40	-	31.01
2	4	HA	208.4	46.72	1524	3751	-	3.81	12.59	9.94	-	26.34
3	3	H	623	148.5	453	-	-	1.23	23.43	-	-	24.66
4	4	HA	723	353	632	2653	-	2.10	8.32	32.60	-	43.02
5	5	HKH	831	162	513	317	2500	0.97	6.63	14.20	18.40	40.20
6	5	KQH	382	1565	189	89.6	7512	0.52	0.71	6.36	41.00	48.59
7	4	KH	521	1503	281	2524	-	1.92	4.51	29.50	-	35.93
8	4	HK	456	127	682	410	-	1.30	9.43	25.70	-	36.43
9	4	QH	524	111.8	19.52	2756	-	0.17	12.32	9.09	-	21.58
10	4	HK	920	104	721	502	-	1.20	15.20	10.90	-	27.30
11	3	H	815	123	653	-	-	1.40	18.63	-	-	20.03
12	3	H	599.8	100	961.3	-	-	1.39	25.48	-	-	26.87

The 2D resistivity imaging survey involves measuring a series of constant separation traverse with the electrode spacing being increased with each successive traverse and thus a combination of lateral profiling and vertical electrical sounding (e.g. Ernstson and Kirsch, 2009; Janik and Krummel, 2009; Singhal and Gupta, 2010; Reynolds, 2011). It was carried out along two traverses: traverse 1 and traverse 2 employing the dipole-dipole electrode configuration. Traverse 1 passes through VES 3 and VES 12, while traverse 2 across VES 4 and VES 5; this approach was used in order to obtain more detailed subsurface hydro-geological information by integrating results from both the vertical electrical sounding (VES) (also known as 1D resistivity sounding) and 2D resistivity imaging. Dipole-dipole configuration was adopted because it is the most useful electrode configuration for measuring both vertical and lateral resistivity variations in the subsurface; it usually gives good quality, as well as detailed, subsurface information in two-dimensional (2D) view (Ward, 1990; Ernstson and Kirsch, 2009; Janik and Krummel, 2009; Reynolds, 2011) and has been widely used in groundwater exploration and/or solving hydrogeological problems as well as geotechnical studies. Current was injected into the subsurface with a current dipole (C1 – C2) and resulting potential difference (voltage gradient) measured using the potential dipole (P1 – P2). The increase in spacing between the current dipole (C1 – C2) and potential dipole (P1 –P2) causes an increase in depth of investigation. Inter-electrode spacing (a) of 10 m was used, with expansion factor (n) varied from 1 to 8. The total length of each transverse profile was 200 m. Apparent resistivity (ρ_a) in ohm-m at each dipole spacing (Barker, 2007; Seidel and Lange, 2007; Anudu *et al*., 2014) was computed using:

$$\boldsymbol{\rho_a = \pi\, a\, n\, (n+1)(n+2)\, R} \quad \text{.....(2)}$$

where a is inter-electrode spacing; n is expansion factor, and R is resistance which is potential difference over current (i.e. $R = \Delta V/I$).

The field measured apparent resistivity data values were plotted on a depth section along intersecting 45^0 point underneath the center of the dipoles (Figure 3) and then subjected to two-dimensional (2D) inversion based on finite element method (FEM) modeling using the DIPRO for Windows Version 4.01 (KIGAM, 2001) software, in order to avoid non-uniqueness solution problems and to generate a high-resolution 2D resistivity section that accurately represent the subsurface geological feature at minimum root mean square (RMS) error. Two main inversion parameters used during the 2D inversion employing the FEM modeling are second-order smoothness constraint and active constraint balancing approach. The second-order smoothness constraint is the spatial derivative order of smoothing method employed during the implementation of smoothness constraint on the resistivity data and its work is to regularise the inversion process. The active constraint balancing approach determines Lagrangian multiplier variable automatically in space domain using the Backus-Gilbert spread function analysis that evaluates the spatial distribution of the row vectors of the parameter resolution matrix as well as its resolving power (Menke, 1984) and it functions as a weighting factor which controls and/ balances the RMS error and smoothness of the structure or feature (Yi and Kim, 1998; Yi *et al*., 2003); hence, gives the optimal resolution of 2D inverted model at depth. The active constraint balancing approach was used, instead of the conventional constant multiplier approach, because it produces optimal, high resolution of the 2D inverted model at greater depth due to its high resolving power (Yi and Kim, 1998) such that the subsurface geological feature/body can clearly be imaged. Maximum possible depth of the 2D inverted model is usually confined to eight times the dipole electrode spacing when active constraint balancing approach is applied, especially if the field measured resistivity data have high signal to noise (S/N) ratio, while it is five times the dipole electrode spacing for constant multiplier approach (KIGAM, 2001). The Jacobian matrix, also known as the sensitivity matrix, was also recalculated at each iteration stage using the Marquardt approach so as to produce a more accurate, stable and rapid inversion process. In this 2D resistivity inversion tasks, eighth iterations were performed because at the eighth iteration with 7.1 % RMS error the field measured resistivity data and the computed (theoretical) resistivity responses tend to remain constant. At completion of all the inversion processes, a 2D resistivity depth section showing the final subsurface resistivity distribution was obtained which represents a high resolution subsurface image of geological features or bodies along the transverse profile (Figure and).

Results and Discussion

Geological Interpretation of the 1D Resistivity Sounding (VES) Results

Interpretation of the 1D resistivity sounding (VES) data curves obtained from the study area showed three to five geoelectrical layers (Figure 3; Table 1), namely:

collapsed zone, highly weathered bedrock, slightly weathered/fractured bedrock and fresh bedrock. Generally, the interpretation of resistivity sounding (VES) data usually gives resistivity models whose layer boundaries are boundaries of geoelectrical but not necessary of geological layers. Therefore for a better delineation of the underlying geology, results from four (4) resistivity soundings (VES 2, 4, 5, and 12) conducted in close proximity to two water boreholes have been correlated with known lithology (Figure 4). Based on the borehole lithological logs from borehole RG01 (Figure 4), the geological interpretation of the geoelectrical model for VES 2 and VES 12 (Figure 4) is : (a) a relatively thick, lateritic sandy clay and/ clayey sand having resistivity values of 208.4 ohm-m (for VES 2) and 599.8 ohm-m (for VES 12) with little moisture content; (b) a thick clayey-sand (i.e. highly decomposed or weathered granite) highly water saturated with a relatively low resistivity value of 46.72 ohm-m (for VES 2) and 100 ohm-m (for VES 12); (c) a slightly weathered/fractured granites (water saturated) with resistivity values of 1524 ohm-m (for VES 2) and 961.3 ohm-m (for VES 12), and (d) a fresh biotite granite rock with high resistivity value of 3751 ohm-m at VES 2. The depth to groundwater level is 5.6 m in borehole RG01, 4.9 m at VES 2 and 5.2 m at VES 12.

Also using the borehole lithological log TR02 (Figure 4), geological interpretation for VES 4 and VES 5 is as follows: (a) a relatively thin lateritic sand layer with variable moisture content and resistivity value of 723 ohm-m (for VES 4) and 831 ohm-m (for VES 5); (b) a relatively thick, water saturated sand to silty-sand layer (highly weathered quartzite/schistose rock) with resistivity value of 353 ohm-m (for VES 4) and 162 ohm-m (for VES 5); (c) a thick fractured quartzite/schistose rock, relatively saturated with water and having resistivity value of 632 ohm-m (for VES 4) and 513 ohm-m (for VES 5), and (d) a fresh quartzite/schistose bedrock with resistivity value of 2653 ohm-m (for VES 4) and 2500 ohm-m (for VES 5). The groundwater level occurs at depth of 5 m in borehole TR02, 4.6 m at VES 4 and 4.8 m at VES 5. Therefore, layer thicknesses and groundwater level (water-table) depths as interpreted from the resistivity sounding data were generally consistent with those observed in the two water boreholes to a good extent (Figure 4).

Geoelectrical Characteristics of the 1D Resistivity Sounding (VES) Results

The three to five geoelectrical layers (Figure 3; Table 1)

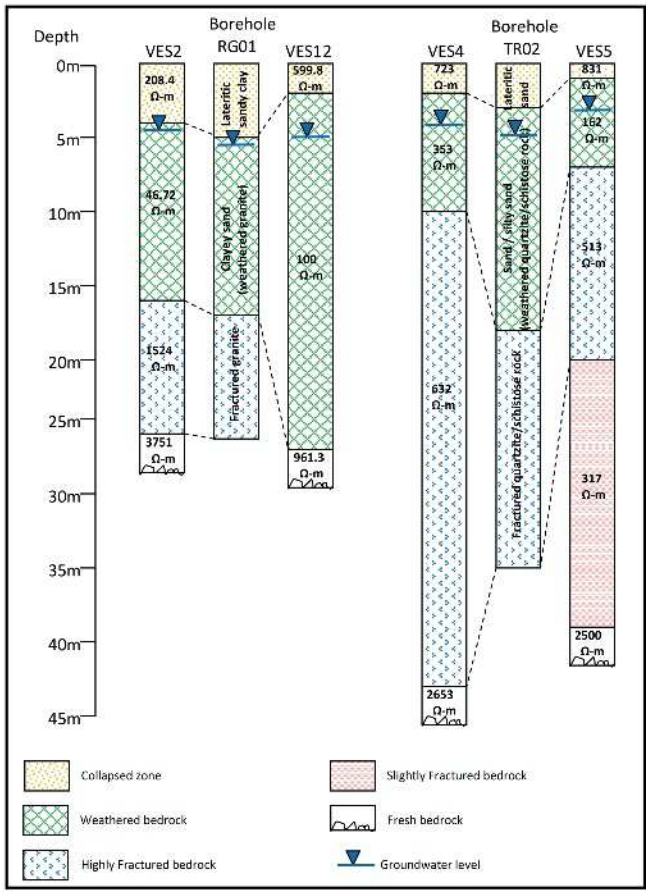

Fig. 4: Correlation of resistivity sounding (VES) results and borehole lithological logs in the area

delineated from the interpretation of the 1D resistivity sounding (VES) data are described as follows: (i) The first layer, referred to as the collapsed zone, chiefly composed of lateritic sands/sandy clays and/ reddish clayey to gravelly sands with thickness of 0.17 to 3.81 m, and resistivity varying from 456 to 920 ohm-m. (ii) The second layer referred to as the highly weathered bedrock; it mainly consists of sandy-clays, clayey-sands, silty-sands and sands with resistivity ranging from 46.72 to 353 ohm-m, and is 0.71 to 25.48 m thick. (iii) The third layer being the slightly weathered/fractured bedrock with resistivity varying from 154 to 1524 ohm-m; it is 6.36 to 32.60 m thick and mainly composed of slightly decomposed/weathered and fractured bedrocks (granites and quartzite/schistose rocks), and (iv) The forth layer referred to as the fresh bedrock (fresh granites and quartzite/schistose rocks); its resistivity ranges between 2500 and 7512 ohm-m. Both the weathered and fractured bedrocks constitute the major aquiferous units (aquifers) in the study area, considering their relatively-low resistivity values and moderately-high thickness values. Most hand-dug and motorised hand-pump wells/boreholes in the area are

abstracting water from these aforementioned aquifer units. Also the fractured bedrock (saprock) aquifers usually occur immediately beneath the weathered bedrock (saprolite) in most locations.

In a three layered earth model, resistivity distribution of subsurface layers can be classified on the basis of 1D resistivity sounding (VES) curve shapes into four types, namely: H-type ($\rho1>\rho2<\rho3$), K-type ($\rho1<\rho2>\rho3$), A-type ($\rho1<\rho2<\rho3$) and Q type ($\rho1>\rho2>\rho3$) (Telford *et al*., 1998); they can also be combined to generate HA-type ($\rho1>\rho2<\rho3<\rho4$), HK-type ($\rho1>\rho2<\rho3>\rho4$), KH-type ($\rho1<\rho2>\rho3<\rho4$), QH-type ($\rho1>\rho2>\rho3<\rho4$) and so on in four layer case, and HKH-type ($\rho1>\rho2<\rho3>\rho4<\rho5$), KQH-type ($\rho1<\rho2>\rho3>\rho4<\rho5$) and so on in five layer case. Hence employing the above-mentioned assertions, the resistivity sounding (1-D) curve types delineated in the study area are H, HA, HK, KH, QH, HKH and KQH (Figure 5; Table 1; Table 2). Furthermore, results derived from statistical analysis (as shown on a pie chart; Figure 5; Table 2) reveals that the H, HA, HK, KH, QH, HKH and KQH constitute 25%, 17%, 17%, 17%, 8%, 8% and 8% of resistivity sounding curves and thus indicating that the dominant resistivity sounding curve types in the study area are H, HA, HK and KH (Figure 5; Table 2). These findings are in good agreement with a number of resistivity sounding studies previously conducted across the crystalline basement complex terrains of Nigeria which identified the H and HA types as the most dominant resistivity sounding curve types (e.g. Aina *et al*., 1996; Olayinka, 1996; Olayinka *et al*., 2000; Anudu et al., 2008, 2011, 2014).

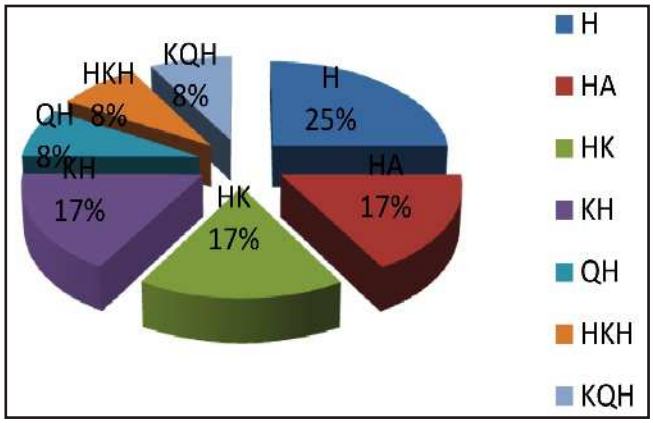

Fig. 5: Pie chart of classification of resistivity sounding (VES) curve types for the area.

Table 2: Summary of the vertical electrical sounding (VES) curve-types for the area.

Curve type	H	HA	HK	KH	QH	HKH	KQH
Frequency	3	2	2	2	1	1	1
Percent (%)	25	17	17	17	8	8	8

Geological Interpretation of the Inverted 2D Resistivity Imaging Sections

The probable geological interpretations of the 2D resistivity imaging sections obtained from the inversion of the dipole-dipole resistivity survey data acquired along traverses 1 and 2 are presented in Figures 6 and 7. Each inverted 2D resistivity imaging section reflects qualitatively both the lateral and vertical variations of the subsurface crustal basement resistivity along the traverse. It gives significant insights about the hydro-geoelectrical characteristics of the subsurface basement lithologies beneath the area. It delineates and image five distinct lithological layers across the area (Figures 6 and 7). The uppermost layer (layer A) consists of lateritic clay with resistivity of about 340 – 400 ohm-m (for traverse 1) and sandy clay to clayey sand with resistivity of about 180 – 398 ohm-m (for traverse 2). It is relatively thin (ca. 1.8 – 2.9 m thick) and represents the collapsed zone (also referred to as soil/mobile zone, duricrust and / mottled zone) which generally results from prolonged dissolution and leaching of weathered bedrock. The second layer (layer B1) composes of highly weathered biotite granite bedrock (upper saprolite unit) characterised by resistivity of 185 – 640 ohm-m (for traverse 1) and a weathered schistose quartzite bedrock (also an upper saprolite unit) with resisivity of 165 – 709 ohm-m (for traverse 2). It is generally more than 3 m thick and slightly water saturated (i.e. an aquiferous unit) in most areas; most hand-dug well in the area are presently abstracting groundwater from it. However, few areas with pockets of relatively high resistivity zones observed around 12 – 14 m profile range and 17 – 19 m profile range (along traverse 1; Figure 6), as well as 3.5 – 5 m profile range together with 17.3 – 19 m profile range (along traverse 2; Figure 7) generally lack water (non-water bearing) and may have resulted from differential weathering of these basement bedrocks. The third layer (layer B2) consists of highly weathered biotite granite and highly weathered schistose quartzite bedrocks (lower saporite units) exhibiting the lowest resistivity values varying from 95 – 344 ohm-m and 81 – 340 ohm-m for traverse 1 and traverse 2, respectively. Its low resistivity nature indicates that it is highly saturated with groundwater. It is also about 10 – 40 m thick and represents the main aquiferous unit; at present, most available deeper wells and boreholes are abstracting groundwater from this lithological layer. The fourth layer (layer C) represents fractured biotite granite and fractured schistose quartzite bedrock layers (saprock) slightly saturated with groundwater and having a resistivity varying from 340 – 700 ohm-m along respective traverses. It is also an

aquiferous unit (fractured aquifer) in the area. Finally, the fifth layer (layer D) exhibits the highest resistivity values ranging from about 700 – 1457 ohm-m and generally indicates fresh bedrocks containing little or no water. It composes of fresh biotite granite and fresh schistose quartzite bedrocks for traverses 1 and 2, respectively and represents an aquiclude (or aquifuge) unit across the area. At this juncture, it important to emphasise that both the weathered and fractured biotite granite/schistose quartzite bedrock layers (labelled B1, B2 and C) generally constitutes the aquiferous units (or aquifers) across the area.

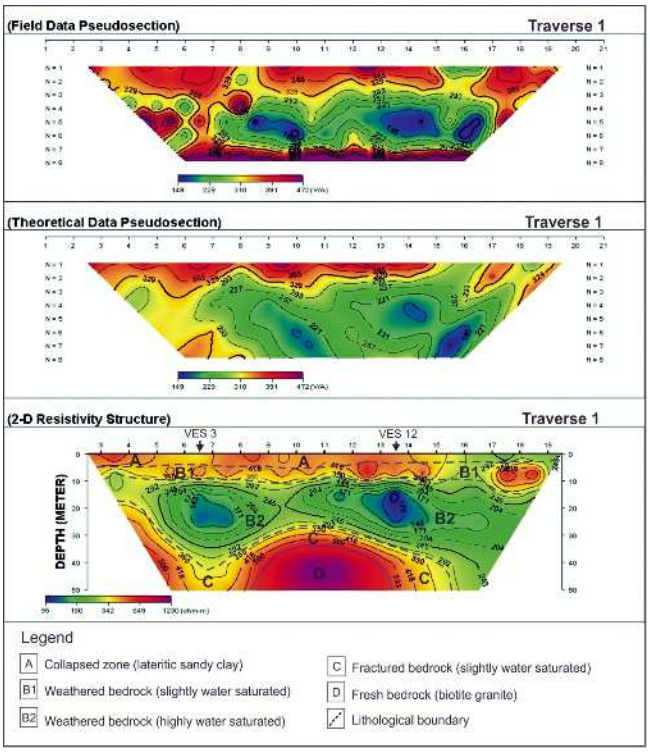

Fig. 6: Interpretation of inverted two-dimensional (2D) resistivity section along traverse 1. Field measured apparent resistivity pseudosection is presented at the top, followed by a theoretical (computed) apparent resistivity pseudosection, and finally, the inverted true 2D resistivity section showing the subsurface geological features or structures in 2D view. The surface elevations were not included during the resistivity inversions because the area has relatively the same topographic reliefs.

Coefficient of Anisotropy Estimation

Coefficient of anisotropy (λ) is one of the important parameters used to define target areas of good groundwater potentials within the crystalline basement complex terrains of Nigeria (e.g. Olorunfemi and Olorunniwo, 1985; Olorunfemi *et al.*, 1991). According to Keller and Frischknecht (1966) and Zohdy *et al.* (1974), the anisotropy coefficient (λ) is given by the equation:

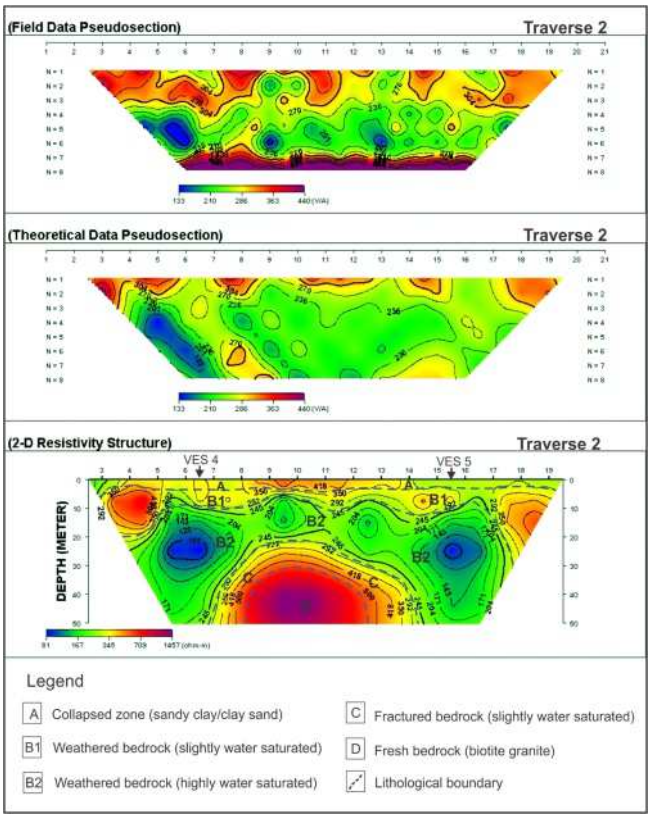

Fig. 7: Interpretation of inverted two-dimensional (2D) resistivity section along traverse 2. Field (measured) apparent resistivity pseudosection is presented at the top, followed by a theoretical (computed) apparent resistivity pseudosection, and finally, the inverted true 2D resistivity section showing the subsurface geological features or structures in 2D view. The surface elevations were not included during the resistivity inversions because the area has relatively the same topographic reliefs

$$\lambda = \sqrt{\frac{T_R S}{H}} \quad \text{.....(1)}$$

Where T_R and S are transverse resistance and longitudinal conductance, respectively, and they are also referred to as Dar Zarrouk parameters; H is overburden thickness (depth to fresh bedrock), which is a summation of thickness values of the collapsed zone, weathered bedrock and fractured bedrock. For isotropic medium, λ = 1, whereas for anisotropic medium, λ > 1. The transverse resistance (T_R) in equation 1 is given as (Maillet, 1947; Keller and Frischknecht, 1966; Zohdy *et al.* 1974):

$$\mathbf{T_R = \sum h_i \rho_i = h_1 \rho_1 + h_2 \rho_2 + \ldots + h_n \rho_n} \quad \text{.....(2)}$$

While the longitudinal conductance (S) is given by the relation (Maillet, 1947; Keller and Frischknecht, 1966; Zohdy *et al.* 1974):

$$\mathbf{S = \sum h_i/\rho_i = (h_1/\rho_1) + (h_2/\rho_2) + \ldots + (h_n/\rho_n)} \quad \text{.....(3)}$$

Where h and ρ are layer thickness and layer resistivity obtained from resistivity sounding interpretation.

The coefficients of anisotropy at each resistivity sounding (VES) points in the area were computed using equation 1. Anisotropy coefficient (λ) values in the area ranged from 1.03 to 2.65 with a mean of 1.31 (Table 3); it depicts that the area generally has good potential basement aquifers (i.e. weathered and fractured bedrocks) characterized by moderate porosity and permeability, and it is expected that the groundwater yields will be moderately high. This interpretation is supported by published results of a number of studies (e.g. Olorunfemi and Olorunniwo, 1985; Olorunfemi *et al.*, 1991) conducted across the basement complex terrains of the southwestern Nigeria which have shown that a direct positive correlation commonly exist between the coefficient of anisotropy of basement rock aquifers and the borehole yields. Also they revealed that the groundwater yields from basement rock aquifers generally increase with increase in coefficient of anisotropy (e.g. Olorunfemi and Olorunniwo, 1985; Olorunfemi *et al.*, 1991). Furthermore, this study also shows that the Precambrian to Lower Paleozoic crystalline basement rocks in the Rogo area are inhomogeneous and anisotropic in nature/character. The anisotropic nature of these crystalline basement rocks can be attributed to near-surface effects, mineralogical composition of bedrock, extensive weathering and variable degree of fracturing.

Table 3: The overburden thickness (depth to fresh bedrock), Dar Zarrouk parameters and coefficient of anisotropy in study area.

VES No	Overburden thickness, H (m)	Longitudinal conductance, S $(ohm)^{-1}$	Transverse resistance, T $(Ohm\text{-}m^2)$	Anisotropy coefficient, λ
1	31.01	0.156	6547.31	1.03
2	26.34	0.294	16530.77	2.65
3	24.66	0.160	4245.65	1.06
4	43.02	0.078	25058.46	1.03
5	40.20	0.128	14997.53	1.09
6	48.59	0.493	6185.43	1.14
7	35.93	0.112	16068.35	1.18
8	36.43	0.115	19317.81	1.29
9	21.58	0.576	1643.89	1.43
10	27.30	0.163	10543.70	1.52
11	20.03	0.153	3432.49	1.15
12	26.87	0.257	3381.72	1.10

Estimation of Aquifer Transmissivity

It is important to estimate the transmissivity (T) of aquifers in any groundwater investigation. Aquifer transmissivity (T) is the ability of an aquifer to transmit fluids through its entire thickness; thus, it is the best aquifer parameter to express groundwater abstraction possibilities. It is usually best determined from borehole or well pumping test data. However, in areas with limited or no pumping test data, aquifer transmissivity may be estimated from the 1D resistivity sounding (VES) data using the Dar Zarrouk parameters (longitudinal conductance S and transverse resistance T_R) (Maillet, 1947; Keller and Frischknecht, 1966; Zohdy *et al.* 1974). The longitudinal conductance (S) is the layer thickness over resistivity (i.e. $S = h/\rho$), whereas transverse resistance (T_R) is layer thickness times resistivity (i.e. $T_R = h\,\rho$). Niwas and Singhal (1981) estimated the aquifer transmissivity analytically from the Dar Zarrouk parameters and stated the following relations:

$$\mathbf{T = K\alpha}\, T_R \quad \text{.....(4)}$$

and

$$\mathbf{T = (KS)/\alpha} \quad \text{.....(5)}$$

Where T is aquifer transmissivity; K is hydraulic conductivity; α is electrical conductivity; T_R is transverse resistance and S is longitudinal conductance.

For this study, the Dar Zarrouk parameters (longitudinal conductance S and transverse resistance T_R) used to compute the aquifer transmissivity (T) were calculated for the weathered aquifer layers delineated from the resistivity sounding (VES) data putting into consideration only the weathered bedrock aquifer resistivity and thickness values (Table 4). Using an average hydraulic conductivity (K) value of 1.3 m/d (Akaolisa, 2006) obtained from a similar geological basement terrain in Nigeria, the aquifer transmissivity (T) values was computed using Equation 5. The Table 4 shows the Dar Zarrouk parameters and aquifer transmissivity (T) values estimated from the resistivity sounding (VES) interpretation results for the weathered bedrock aquifers across the study area. The computed weathered bedrock aquifer transmissivity (T) in the study area varied from 16.01 to 53.30 m^2/day (Table 4) with an average aquifer transmissivity value of 30.91 m^2/day. Umego *et al.* (2000) and Akaolisa (2006) working in a similar geological terrains in Nigeria obtained an average aquifer transmissivity value of 25 m^2/day and 26 m^2/day, respectively. Using the Krásný (1993) transmissivity classification, 100 % (i.e. all) of the aquifer transmissivity values computed in the study area are within the Class III and have intermediate (or moderately high) transmissivity (Table 5). Therefore, weathered bedrock aquifers delineated have moderately high transmissivity and could transmit enough water to

wells/boreholes which can be economically abstracted to satisfy the domestic and/or agricultural needs of the people in the area. Hence, the findings of this study show that the area generally has good groundwater potentials.

Table 4: Summary of Dar Zarrouk parameters and aquifer transmissivity (T) estimated for the weathered aquifers in the area.

VES No	Aquifer resistivity, ρ (ohm-m)	Aquifer thickness, h (m)	Electrical conductivity, α (ohm-m)$^{-1}$	Longitudinal conductance, S (ohm)$^{-1}$	Transverse resistance, T_R (ohm-m^2)	Transmissivity, T (m^2/day)
1	258	16.32	0.00388	0.06322	4207.98	21. 20
2	46.72	12.59	0.02140	0.26948	588.21	16.37
3	148.5	23.43	0.00673	0.15778	3479.36	30.48
4	632	32.60	0.00158	0.05158	20603.20	42.43
5	415	32.60	0.00241	0.07856	13529.00	42.38
6	89.6	41.00	0.01116	0.45759	3673.60	53.30
7	281	29.50	0.00356	0.10498	8289.50	38.34
8	682	25.70	0.00147	0.03768	17527.40	33.32
9	111.8	12.32	0.00895	0.11020	1377.38	16.01
10	104	15.20	0.00962	0.14615	1580.80	19.75
11	123	18.63	0.00813	0.15146	2291.49	24.22
12	100	25.48	0.01000	0.2548	2548.00	33.13

Table 4: Summary of Dar Zarrouk parameters and aquifer transmissivity (T) estimated for the weathered aquifers in the area.

Transmissivity (m^2/d)	Class	Designation	Groundwater supply potential	Percentage of transmissivity computed for the study area
> 1000	I	Very high	Withdrawals of great regional importance	_
100 – 1000	II	High	Withdrawals of lesser regional importance	_
10 – 100	III	Intermediate	Withdrawals for local water supply (small communities, plants, etc.)	100
1 – 10	IV	Low	Smaller withdrawals for local water supply (private consumption, etc.)	_
0.1 – 1	V	Very low	Withdrawals for local water supply with limited consumption	_
< 0.1	VI	Imperceptible	Sources for local water supply are difficult (if possible) to ensure	_

Correlation of Computed Aquifer Transmissivity, Transverse Resistance and Anisotropy Coefficient

The computed aquifer transmissivity (T) and aquifer transverse resistance (T_R) for each resistivity sounding point in the study area were plotted on a scatter graph as shown in Figure 8. A weak positive correlation is found between the two variables (least square regression, correlation coefficient R^2 = 0.493), indicating that the water transmitting capacity of the potential basement aquifers will moderately increase as the transverse resistance increases.

In addition, the correlation between anisotropy coefficient (λ) and the aquifer transmissivity (T) of the weathered bedrock (Figure 9) showed a weak negative relationship, with correlation coefficient (R^2) of 0.380; it depicts that 38 % of variance in weathered aquifer transmissivity is explained by the anisotropy coefficients obtained for the crystalline basement rocks. Thus, it can generally be inferred that the anisotropic nature of the crystalline basement rocks affects the transmissivity of the weathered bedrock aquifer across the area.

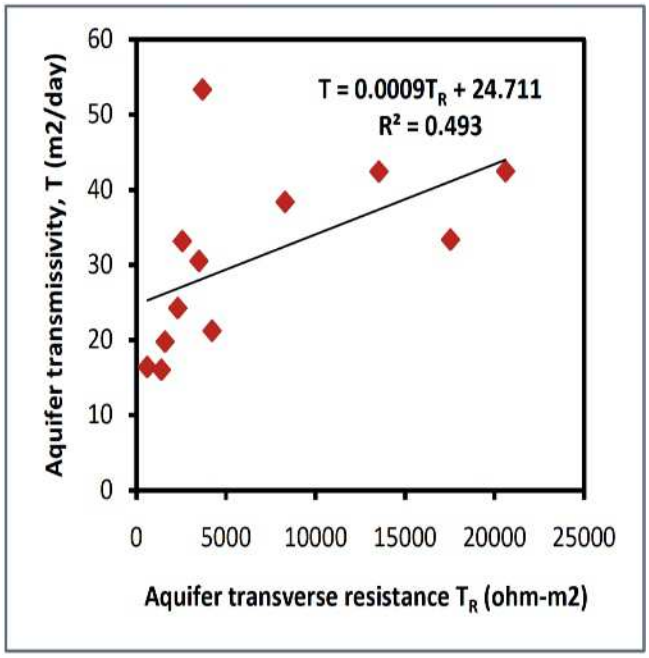

Fig. 8: Relationship of transverse resistance T_R (ohm-m^2) of the weathered bedrock aquifer with its aquifer transmissivity T (m^2/day). A weak positive correlation (R^2 = 0.493) suggests that the computed aquifer transverse resistance will exerts a moderate control on the computed aquifer transmissivity.

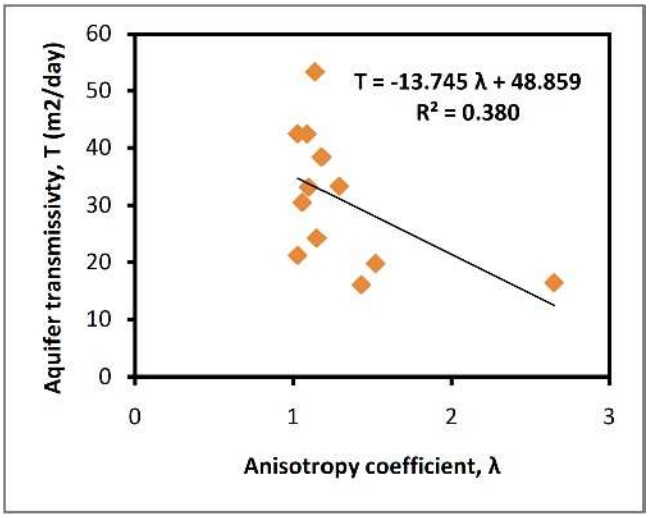

Fig. 9: Relationship between the coefficient of anisotropy λ and the aquifer transmissivity T (m^2/day) of the weathered bedrock.

Conclusions

The application of resistivity soundings was investigated for the purpose of delineating geoelectrical parameters and potential basement aquifers, as well as estimating the aquifer transmissivity of the weathered bedrock. Results showed that three to five geoelectrical layers exist in the area, with the weathered and fractured zones in the bedrocks being the aquifers. Coefficient of anisotropy (λ) values obtained varied from 1.03 to 2.65 with a mean value of 1.31, while the calculated aquifer transmissivity (T) of the weathered bedrock ranged from 16.01 to 53.30 m^2/day with an average aquifer transmissivity value of 30.91 m^2/day. This study shows that the Rogo area generally has good groundwater potentials.

References

Adefolalu, A.O. (2002). Climate. In: Africa Atlases; Atlas of Nigeria. Les Editions J. A. Aux E'dition du Jaguar 57 bis, rue d'Auteuil-75016 Paris-France.

Ahmed, S., Marsily, G.D. and Talbot, A. (1988). Combined use of hydraulic and electrical properties of aquifer in a geostatistical estimation of transmissivity. Groundwater, Vol. 26, No. 1, Pp. 78-86.

Aina, A., Olorunfemi, M.O. and Ojo, J.S. (1996). An integration of aeromagnetic and electrical resistivity methods in dam site investigation. Geophysics, Vol. 61, Pp. 349-356.

Anudu, G. K., Onwuemesi, A. G., Ajaegwu, N. E., Onuba, L. N. and Omali, A. O. 2008. Electrical resistivity investigation for groundwater in the basement complex terrain: A case study of Idi-Ayunre and its environs, Oyo State, southwestern Nigeria. Natural and Applied Sciences Journal, Vol. 9, No. 2, Pp. 1-12.

Anudu, G.K., Onuba, L.N. and Ufondu, L.S. (2011). Geoelectric sounding for groundwater exploration in the crystalline Basement Complex terrain around Onipe and adjoining areas, southwestern Nigeria. Journal of Applied Technology in Environmental Sanitation, Vol. 1, No. 4, Pp. 343-354.

Anudu, G.K., Essien, B.I. and Obrike, S.E. (2014). Hydrogeophysical investigation and estimation of groundwater potential of the Lower Palaeozoic to Precambrian crystalline basement rocks in Keffi area, north-central Nigeria, using resistivity methods. Arabian Journal of Geosciences. Vol. 7. Pp. 311-322.

Akaolisa, C. (2006). Aquifer transmissivity and basement structure determination using resistivity sounding at Jos Plateau State Nigeria. Environmental Monitoring and Assessment, Vol. 114, Pp. 27-34.

Bala, A.E. and Ike, E.C. (2001). The aquifer of the crystalline basement rocks in Gusau area, northwestern Nigeria. Journal of Mining and Geology, Vol. 37, No. 2, Pp. 177-184.

Barker, R, Blunk, I. And Smith, I. 1996. Geophysical consideration in the design of UK National Resistivity Sounding Database. First Break, Vol. 14, No. 2, Pp. 45-53.

Barongo, J.O. and Palacky, G.J. (1991). Investigation of electrical properties of weathered layers in the Yala area, western Kenya, using resistivity soundings. Geophysics, Vol. 56, No. 1, Pp. 133-138.

Batte, A.G., Muwanga, A., Sigrist, P.W. and Owor, M. (2008). Vertical electrical sounding as an exploration technique to improve on the certainty of groundwater yield in the fractured crystalline basement aquifers of eastern Uganda. Hydrogeology Journal, Vol. 16, Pp. 1683-1693.

Bernard, J. (2003). Short note on depth of investigation of electrical methods. www.iris-instruments.com. Web accessed 27th July 2006.

Bobachev, A.A. (2002). IPI2Win version 3.0.1: A windows software for an automatic interpretation of resistivity sounding data, Ph.D., Moscow State University.

Chandra, S., Ahmed, S., Ram, A. and Dewandel, B. (2008). Estimation of hard rock aquifer hydraulic conductivity from geoelectrical measurements: A theoretical development with field application. Journal of Hydrology, Vol. 357, Pp. 218-227.

David, L.M. (1988). Geoelectric study of shallow hydrogeological parameters in the area around Idere, southwestern Nigeria. Unpublished PhD Thesis, University of Ibadan.

Dan-Hassan, M.A. and Olorunfemi, M.O. (1999). Hydrogeophysical investigation of a basement terrain in the north-central part of Kaduna State Nigeria. Journal of Mining and Geology, Vol. 35, No.2, Pp. 189-205.

Dentith, M. and Mudge, S.T. (2014). Geophysics for the mineral exploration geoscientist. Cambridge University Press, Cambridge, United Kingdom. 426p.

Dhakate, R. and Singh, V.S. (2005). Estimation of hydraulic parameters from surface geophysical methods, Kaliapani Ultramafic Complex, Orissa India. Journal of Environmental Hydrology, Vol. 13, No. 12.

De Lima, O.A.L. and Niwas, S. (2000). Estimation of hydraulic parameters of shaly sandstone aquifers from geologic measurements. Journal of Hydrology, Vol. 235, Pp. 12-26.

Ernstson, K. and Kirsch, R. (2006). Geoelectrical methods. In Groundwater geophysics – a tool for hydrogeology, 1st edition, (Kirsch, R. ed.), Springer, Berlin, Pp. 85-118.

Ernstson, K. and Kirsch, R. (2009). Geoelectrical methods. In Groundwater geophysics – a tool for hydrogeology, 2nd edition, (Kirsch, R. ed.), Springer, Berlin, Pp. 85-109.

Frohlich, R. and Kelly, W.E. (1985). The relation between transmissivity and transverse resistance in a complicated aquifer of glacial outwash deposits. Journal of Hydrology, Vol. 79, Pp. 215-219.

Gowd, S.S. (2004). Electrical resistivity surveys to delineate groundwater potential aquifers in Peddavanka watershed, Anantapur District, Andhra Pradesh, India. Environmental Geology, Vol. 46, Pp. 118-131.

Hazell, J.R.T., Cratchley, C.R. and Jones, C.R.C. (1992). The hydrogeology of crystalline aquifers in northern Nigeria and geophysical techniques used in their exploration. In: Wright, E.P. and Burgess, W.G. (eds.). The hydrogeology of crystalline basement aquifers in Africa. Geological Society Special Publication, No.66, Pp. 155-182.

Hubbard, S. H. and Rubin, Y. (2002). Hydrogeological parameter estimation using geophysical data: A review of selected techniques. Journal of Contaminant Hydrology, Vol. 45, Pp. 3-34.

Janik, M. and Krummel, H. (2009). 2D measurements in Geoelectrical methods. In Groundwater geophysics – a tool for hydrogeology, 2nd edition, (Kirsch, R. ed.), Springer, Berlin, Pp. 109 -117

Keller, G.V. and Frischnecht, F.C. (1966). Electrical methods in geophysical prospecting. Pergamon Press, Oxford, 523p.

KIGAM. (2001). DIPRO for Windows version 4.01. Processing and interpretation sorfware for electrical resistivity data. KIGAM, Daejeon.

Kosinki, W.K. and Kelly, W.E. (1981). Geoelectric sounding for predicting aquifer properties. Groundwater, Vol. 19, Pp. 163-171.

Krásný, J. (1993). Classification of transmissivity magnitude and variation. Groundwater, Vol. 31, No. 2, Pp. 230-236.

Maillet, R. (1947). The fundamental equations of electrical prospecting. Geophysics, Vol. 12, Pp. 529-556.

Mbipom, E.W., Okwueze, E.E. and Onwuegbuche, A.A. (1996). Estimation of transmissivity using VES data from Mbaise area of Nigeria. Nigerian Journal of Physics, Vol. 85, Pp. 28-32.

Mbonu, P.D.C., Ebeniro, J.O., Ofoegbu, C.O. and Ekine, A.S. (1991). Geoelectric sounding for determination of aquifer characteristics in parts of Umuahia area of Nigeria. Geophysics, Vol. 56, Pp. 284-291.

Menke, W. (1984). Geophysical data analysis: discrete inverse theory. Academic, Orlando.

Niwas, S. and Singhal, D.C. (1981). Estimation of aquifer transmissivity from Dar-Zarrouk parameters in porous media. Journal of Hydrology, Vol. 50, Pp. 393-399.

Niwas, S. and Singhal, D.C. (1985). Aquifer transmissivity of porous media from resistivity data. Journal of Hydrology, Vol. 82, Pp. 143-153.

Niwas, S. and De Lima, O.A.L. (2003). Aquifer parameter estimation from surface resistivity data. Groundwater, Vol. 41, No. 1, Pp. 94-99.

Offodile, M.E. (1983). The occurrence and exploitation of groundwater in Nigerian basement rocks. Nigerian Journal of Mining and Geology, Vol. 20, No. 1 & 2. Pp. 131-146.

Onuoha, K.M. and Mbazi, F.C.C. (1988). Aquifer transmissivity from electrical sounding data of the case of Ajali Sandstone aquifers, southeast of Enugu, Nigeria. In: C. O. Ofoegbu (ed.). Groundwater and Mineral Resources of Nigeria. Friedvieweg and Sons Pub. Berlin, Germany. Pp. 17-29.

Olayinka, A.I. (1996). Non-uniqueness in the interpretation of bedrock resistivity from sounding curves and its hydrogeological implications. Water Resources, Vol. 7, Nos. 1 & 2, Pp. 49-55.

Olayinka, A.I., Akpan, E.J. and Magbagbeola, O.A. (1997). Geoelectric sounding for estimating aquifer potential in the crystalline basement area around Shaki, southwestern Nigeria. Water Resources, Vol. 8, Nos. 1 & 2, Pp. 71-81.

Olayinka, A.I., Obere, F.O. and David, L.M. (2000). Estimation of longitudinal resistivity from Schlumberger sounding curves. Journal of Mining and Geology, Vol. 36, No.2, Pp. 225-242.

Olayinka, A.I. and Olorunfemi, M.O. (1992). Determination of geoelectrical characteristics in Okene area and implication for borehole siting. Journal of Mining and Geology, Vol. 28, Pp. 403-412.

Olorode, O. (2002). Vegetation and fauna. In: Africa Atlases; Atlas of Nigeria. Les Editions J. A. Aux E'dition du Jaguar 57 bis, rue d'Auteuil-75016 Paris-France.

Olorunfemi, M.O. and Fasuyi, S.A. (1993). Aquifer types and the geoelectric/hydrogeologic characteristics of part of the central basement terrain of Nigeria (Niger State). Journal of African Earth Sciences, Vol. 16, No.3, Pp. 309-331.

Olorunfemi, M.O. and Olorunniwo, M.A. (1985). Geoelectric parameter and aquifer characteristics of some parts of southwestern Nigeria. Geologia Applicata Indrogeologia, Vol. 20, Pp. 99-109.

Olorunfemi, M.O., Olarewaju, V.O. and Alade, O. (1991). On the electrical anisotropy and groundwater yield in a basement complex area of SW Nigeria. Journal of African Earth Sciences, Vol. 12, No. 3, Pp. 467-472.

Reynolds, J.M. (2011). An introduction to applied and environmental geophysics, 2nd edition. John Wiley & Sons, Ltd, West Sussex, United Kingdom. 696p.

Roy, A. and Apparao, A. (1971). Depth of investigation in direct current methods. Geophysics, Vol. 36, No. 5, Pp. 943-959.

Seidel, K and Lange, G. (2007). Direct current resistivity method. In: Knodel, K, Lange, G. and Voigt, H. J. (eds.) Environmental geology: handbook of field methods and case studies. Springer, Berlin, 1339p.

Singhal, B.B.S. and Gupta, R.P. (2010). Applied hydrogeology of fractured rocks, 2nd edition. Springer, Netherlands, 401p.

Taylor, G. and Eggleton, R.A. (2001). Regolith geology and geomorphology. Wiley, Chichester, 379p.

Telford, W.M., Geldart, L.P. and Sheriff, R.E. (1998). Applied geophysics, 2nd edn., Cambridge University Press, New York. 770p.

Umego, M.N., Zume, J.T. and Ajayi, C.O. (2000). Resistivity sounding for determination of basement structure and aquifer transmissivity. 23rd NIP Annual Conf. Proc. Pp. 181-186.

Yadav, G.S. and Abolfazi, H. (1998). Geoelectrical soundings and their relationship to hydraulic parameters in semiarid regions of Jalore, northwestern India. Journal of Applied Geophysics, Vol. 39, Pp. 35-51.

Yi, M.J. and Kim, J.H. (1998). Enhancing the resolving power of the least squares inversion with Active Constraint Balancing: SEG Expanded Abstracts, 68 Annual Meeting, New Orleans, Pp. 485-488.

Yi, M.J., Kim, J.H. and Chung, S.H. (2003). Enhancing the resolving power of the least-squares inversion with active constraint balancing. Geophysics, Vol. 68, Pp. 931-941.

Ward, S.H. (1990). Resistivity and induced polarisation methods. In: Geotechnical and Environmental Geophysics, S.H., Ward (ed). Investigations in geophysics No. 5, Volume 1: Review and tutorial. Society of Exploration Geophysics, Tulsa, Oklahoma, Pp. 147-189.

White, C.C., Houston, J.F.T. and Barker, R.D. (1988). The Victoria Province drought relief project 1. Geophysical siting of boreholes. Groundwater, Vol. 26, pp. 309-316.

Wright, E.P. (1992). The hydrogeology of crystalline basement aquifers in Africa. Geological Society London, Special Publication, Vol. 66, Pp. 1-27.

Zohdy, A.A.R., Eaton, G.P. and Mabey, D.R. (1974). Application of surface geophysics to groundwater investigations. US Geological Survey, Reston, USGS-TWRI, Book 2, Chapter D1.